ELSEVIER

Surface Science 440 (1999) L863–L867

surface science

www.elsevier.nl/locate/susc

Surface Science Letters

A simplified but intuitive analytical model for intermittent-contact-mode force microscopy based on Hertzian mechanics

Hartmut Bielefeldt *, Franz J. Giessibl

Experimentalphysik VI, Center for Electronic Correlations and Magnetism, Institute of Physics, Augsburg University,
D-86135 Augsburg, Germany

Received 3 May 1999; accepted for publication 19 June 1999

Abstract

The forces acting on the substrate in intermittent-contact-mode (IC mode, tapping mode) atomic force microscopy are not accessible to a direct measurement. For an estimation of these forces, a simple analytical model is developed by considering only the shift of the cantilever resonance frequency caused by Hertzian (contact) forces. Based on the relationship between frequency shift and tip–sample force for large-amplitude frequency-modulation atomic force microscopy, amplitude and phase versus distance curves are calculated for the intermittent contact mode, and the forces on the substrate are calculated. The results show a qualitative agreement with numerical calculations, yielding typical maximal forces of 50–150 nN. When working above the unperturbed resonance, forces are found to be significantly larger than below the resonance. © 1999 Elsevier Science B.V. All rights reserved.

Keywords: Atomic force microscopy; Intermittent contact; Tapping mode

Intermittent-contact-mode (also known as tapping mode) atomic force microscopy (IC-AFM) is a widespread method for obtaining high-resolution topography images in ambient conditions. Theoretical descriptions of this mode have been published [1–10] based on numerical models. However, a direct and intuitive connection between the operating parameters and the forces involved has been lacking.

Recently, considerable progress was achieved by the solution of the relationship between forces and the resulting frequency shift in frequency-modulation atomic force microscopy (FM-AFM) for several different classes of force laws [11]. In FM-AFM the cantilever is subject to a positive feedback keeping the oscillation amplitude constant, and the frequency of the resonant oscillation is the imaging signal. The measurement of repulsive forces under ambient conditions by FM-AFM was found to be in good agreement with the predictions of Hertzian theory [12].

In IC-AFM the cantilever is driven with a fixed frequency f and excitation amplitude, measuring the resulting oscillation amplitude at this frequency. If the dominant contribution to the IC-AFM signal is due to repulsive tip–sample interaction, it should be possible to describe the system based on the theory for FM-AFM: the

---

* Corresponding author. Fax: +49-821-598-3652.
E-mail address: hartmut.bielefeldt@physik.uni-augsburg.de (H. Bielefeldt)

PII: S0039-6028(99)00861-4

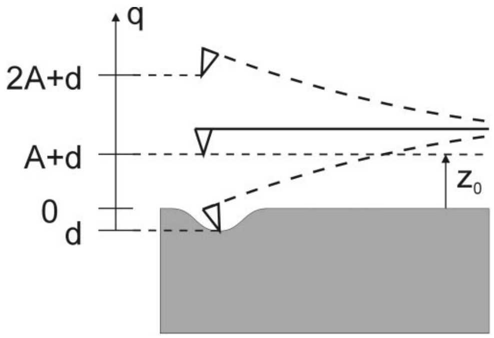

Fig. 1. Schematic illustration of the cantilever oscillating with amplitude A in a distance z_0 above the sample surface. For contact forces, the smallest tip–sample distance is the negative indentation.

interaction increases the cantilever's resonant frequency, and this shift causes a change of the measured amplitude at the excitation frequency. In this paper, this simple model is used to calculate amplitude and phase versus distance curves, and the indentation depth and Hertzian forces involved are estimated. The results show a qualitative agreement with numerical simulations and exhibit a variety of phenomena reported previously [1–10]: the existence of a maximum peak force at amplitude ratios of typically 1/2 [3], peak forces of 50–150 nN for common experimental conditions [6], and generally higher forces [1] and a hysteresis and discontinuity in the amplitude versus distance curves [4,9] for excitation frequencies above the resonance.

The cantilever is characterized by its unperturbed resonance frequency f_0, spring constant k, and quality factor Q. The tip is assumed to be spherical with radius R_{tip}, and the tip–sample interaction is modeled by the Hertzian force for a sphere-plane geometry [13]:

$$F_{\text{tip–sample}}=\begin{cases}\frac{4}{3}\,E^{*}\sqrt{R_{\text{tip}}}|q|^{3/2} & q<0\\ 0 & q\geq 0\end{cases}, \tag{1}$$

with E^{*} being the effective Young's modulus of the tip/sample material combination, and q the distance between sphere and sample. Fig. 1 sketches the geometry and the variables used.

If the forces acting between tip and sample are small compared with the cantilever restoring force ($F_{\text{tip–sample}} \ll kA$) and if the oscillation amplitude is large compared with the range of the forces ($A \gg |d|$), the resonance of the cantilever oscillating with amplitude A increases from its unperturbed frequency f_0 to $f_1=f_0+\Delta f$, and the frequency change can be calculated using first-order Hamilton–Jacobi perturbation theory [11,12,14] as:

$$\Delta f=\begin{cases}\dfrac{f_0}{kA^{3/2}}\,\dfrac{E^{*}\sqrt{R_{\text{tip}}}}{2\sqrt{2}}|d|^{2} & d<0\\ 0 & d\geq 0\end{cases}. \tag{2}$$

To maintain consistency with the notation in Refs. [11,12,14], the value of d for contact forces as described in this paper is negative; the sample is indented by $|d|$. The position z_0 around which the cantilever oscillates is given by $z_0=A+d$; this distance can be varied by the experimentalist, while d is not directly observable in IC mode.

The frequency dependence of the cantilever amplitude in IC mode is modeled by a Lorentz curve:

$$A(f)=\frac{A_{\text{excitation}}Q\times(f_1/f)}{\sqrt{Q_2[(f_1/f)-(f/f_1)]^2+1}}, \tag{3}$$

with quality factor $Q \gg 1$. The driving frequency f is usually chosen close to the unperturbed resonance.

For simplicity, it is assumed that the quality factor of the interacting cantilever is not changed by the interaction, and the calculation is limited to Hertzian forces as the only interaction between tip and sample. These simple assumptions limit the applicability of the model but help to gain insight into the basic mechanisms of the IC mode.

A self-consistent solution of Eqs. (2) and (3) yields an amplitude versus distance curve $A(z_0)$. Since none of the two variables A and f_1 can be eliminated directly, numerical methods would have to be employed. However, another way of calculating an amplitude versus distance curve is an indirect approach. Instead of calculating A and f_1 for a given z_0, we begin with an assumption of amplitude A at the fixed driving frequency f, calculate the perturbed resonance frequency f_1 ($f_1>f_0$) and the corresponding frequency shift Δf. Eq. (2) can be inverted to give the indentation depth d, and $z_0 = A + d$ yields the z_0 position that is compatible with the assumed amplitude A. Performing this calculation for a variety of amplitudes between 0 and the unperturbed amplitude $QA_{\mathrm{excitation}}$ results in a complete amplitude versus distance curve; i.e., the set of pairs (A, z_0) that fulfil Eqs. (2) and (3). The Hertzian force can be calculated from d using Eq. (1).

For driving frequencies not higher than the unperturbed resonance $f \leq f_0$, there is one unique and stable positive solution for Δf, and the curves for tip–sample approach and retraction are the same.

If the driving frequency is larger than the unperturbed resonance frequency, there are two possible positive solutions for Δf. For common experimental parameters, the solution on the high-frequency branch of the Lorentz curve is unstable because $(\partial A/\partial f_1) > -(\partial d/\partial f_1)$: on the onset of the interaction during tip–sample approach (frequency begins to shift to higher values), the amplitude would *increase*, but the indentation depth is too small to compensate this increase in order to comply with the externally adjusted distance z_0. Therefore, the system must discontinuously switch to the solution on the low-frequency branch. During tip retraction, the system can follow the low-frequency branch until the resonance amplitude is reached, and for larger distance z_0 the tip loses contact with the sample.

For an example calculation, we use the parameters of the simulation in Ref. [3]: $k = 20\ \mathrm{N\,m^{-1}}$, $f_0 = 200$ kHz, $Q = 500$, $QA_{\mathrm{excitation}} = 100$ nm, $R_{\mathrm{tip}} = 20$ nm, $E^* = 77 \times 10^9\ \mathrm{N\,m^{-2}}$. Calculations are performed in the manner described above, yielding amplitude, indentation depth, Hertzian force and phase as a function of the externally adjusted distance z_0 of the center of the oscillation. Besides the situation on resonance as discussed in Ref. [3], also the curves for excitation frequency slightly lower and slightly higher than the cantilever free resonance are shown in Figs. 2–4. For the parameters given above, the perturbative approach is well justified for amplitudes larger than about 20–30 nm.

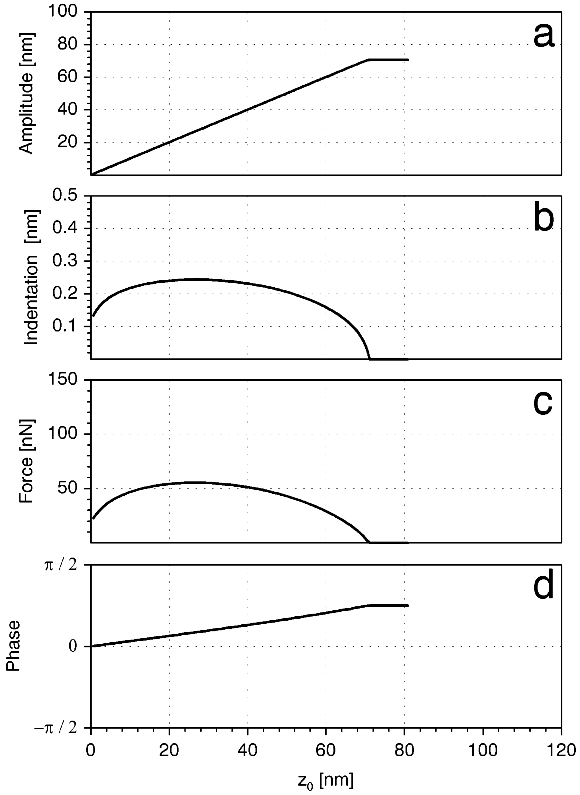

Fig. 2. Frequency chosen below the unperturbed resonance (f= 199.8 kHz): (a) amplitude, (b) indentation depth, (c) force and (d) phase as a function of distance z_0 between sample surface and center of tip oscillation. Parameters for Figs. 2–4 are the same for all three figures: $k = 20\ \mathrm{N\,m^{-1}}$, $f_0 = 200$ kHz, $Q = 500$, $QA_{\mathrm{excitation}} = 100$ nm, $R_{\mathrm{tip}} = 20$ nm, $E^* = 77 \times 10^9\ \mathrm{N\,m^{-2}}$.

For driving frequencies below the resonance (Fig. 2), the amplitude decreases almost linearly with decreasing distance. Force and indentation depth do not reveal a strong variation throughout amplitudes from 10 to 50 nm, and the maximum force reaches 55 nN.

If the driving frequency is the unperturbed resonance frequency (Fig. 3), the traces appear similar, but force and indentation increase rapidly with the beginning of amplitude reduction. In this case, the maximum force is 83 nN. This result can be compared directly with Figs. 3, 4 and 7 of Ref. [3] where the data are given as average force and indentation. These data were rescaled to maximum force and indentation and included as open triangles. Considering the simplicity of the analytical approach, a surprisingly good agreement with the numerical results can be seen.

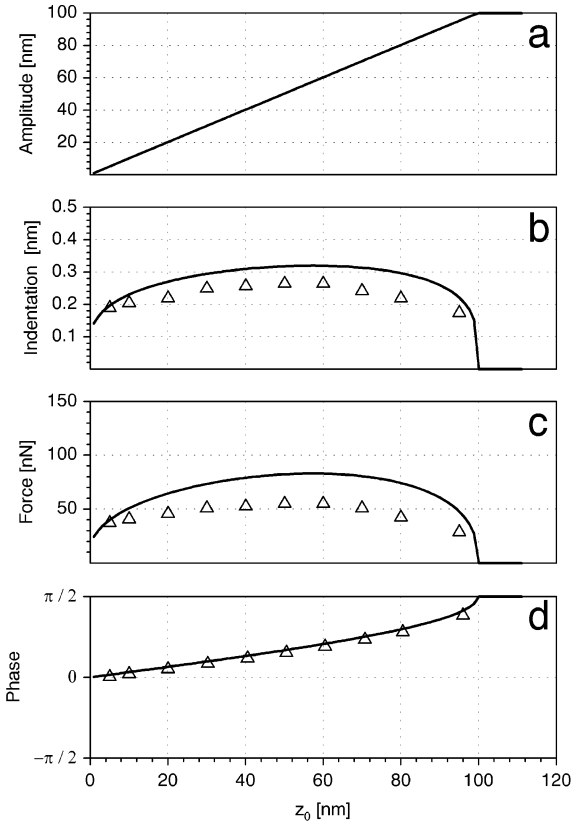

Fig. 3. Frequency chosen on the unperturbed resonance ($f=$ 200 kHz); symbols as in Fig. 2. The corresponding force, indentation and phase values from Ref. [3] are included as open triangles.

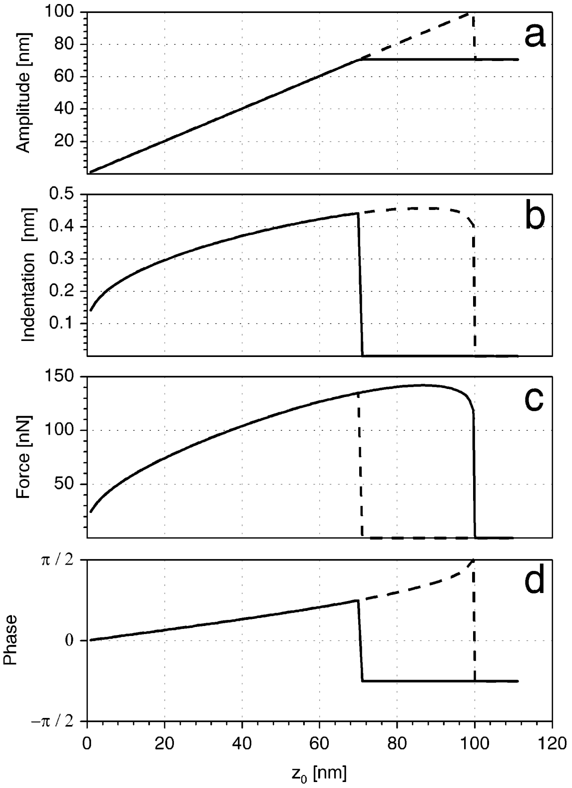

Fig. 4. Frequency chosen above the unperturbed resonance ($f=$ 200.2 kHz). Traces for approach (solid lines) and retraction (dotted lines) show a remarkable difference.

When working above the resonance frequency, tip approach and retraction traces are expected to show a difference (Fig. 4). On approach (solid line), the amplitude remains constant until the interaction starts and decreases (almost) linearly. Indentation and force discontinuously reach values higher than in the case of Figs. 2 and 3. On retraction (dotted lines), the amplitude increases beyond the value that was set in the beginning of the experiment, and reaches the resonant value ($A=100$ nm) before the contact to the sample is lost and the original amplitude is found for larger distance. This hysteresis was found in numerical calculations as well as in the experiment [4]. If the distance z_0 is kept constant and the frequency is sweeped from low to high frequency, this effect leads to a hysteresis on the high-frequency side of the resonance, as it was observed by Bachelot et al. [9] for relatively large oscillation amplitudes where the Hertzian forces are large compared with attractive contributions to the interaction. Indentation and force values on the retraction trace are even larger than during approach. The maximum force value is in the range of 140 nN in this case; i.e., about three times as high as below the resonance. This tendency was already discovered from numerical simulations [1,2].

In summary, the simple analytical model introduced in this paper gives an intuitive picture of the intermittent contact mode with relatively stiff cantilevers on rigid samples. Unlike previous studies involving numerical simulations of the equation of motion, the distance characteristics of amplitude, phase, indentation and force can directly be calculated, and parameters can easily be varied, e.g., in a spreadsheet calculation. For any experimental situation (given cantilever data and choice of excitation frequency and excitation amplitude), the combination of the amplitude and force curves (Figs. 2–4a and 2–4c, respectively) gives an estimate of the force as a function of the amplitude ratio (i.e., of the setpoint that is adjusted by the operator).

The validity of the model is limited by the applicability of Hertzian mechanics as the dominating interaction mechanism; for this case it gives a reasonable estimate of the forces involved. Compared with the typical forces used in contact AFM (a few nN), the forces during intermittent contact are considerably larger and depend strongly on the choice of the excitation frequency. The occurrence of an amplitude hysteresis for frequencies above the cantilever free resonance can easily be understood as a consequence of the repulsive forces.

An extension to more general forces appears to be feasible since the frequency shift in FM-AFM can be calculated in a very general fashion [11]. In such a general case, however, the inversion of Eq. (2) is not easily possible, and it could again become necessary to use numerical methods.

Acknowledgements

Fruitful discussions with S. Hembacher and J. Mannhart are gratefully acknowledged. This work was supported by the BMBF (project number 13N6918/1).

References

[1] J.P. Spatz, S. Sheiki, M. Möller, R.G. Winkler, P. Reineker, O. Marti, Nanotechnol. 6 (1996) 40.
[2] R.G. Winkler, J.P. Spatz, S. Sheiko, M. Möller, P. Reineker, O. Marti, Phys. Rev. B 54 (1996) 8908.
[3] J. Tamayo, R. García, Langmuir 12 (1996) 4430.
[4] B. Anczykowski, D. Krüger, H. Fuchs, Phys. Rev. B 53 (1996) 15485.
[5] D. Krüger, B. Anczykowski, H. Fuchs, Ann. Phys. 6 (1997) 341.
[6] N.A. Burnham, O.P. Behrend, F. Oulevey, G. Gremaud, P.-J. Gallo, D. Gourdon, E. Dupas, A.J. Kulik, H.M. Pollock, Nanotechnol. 8 (1997) 67.
[7] O.P. Behrend, F. Oulevey, D. Gourdon, E. Dupas, A.J. Kulik, G. Gremaud, N.A. Burnham, Appl. Phys. A 66 (1998) 219.
[8] A. Kühle, A.H. Sørensen, J. Bohr, J. Appl. Phys. 81 (1997) 6562.
[9] R. Bachelot, P. Gleyzes, A.C. Boccara, Probe Microsc. 1 (1997) 89.
[10] G. Bar, R. Brandsch, M.H. Whangbo, Surf. Sci. 411 (1998) 802.
[11] F.J. Giessibl, H. Bielefeldt, Phys. Rev. Lett. (1999) submitted for publication.
[12] F.J. Giessibl, Appl. Phys. Lett. 73 (1998) 3956.
[13] C.J. Chen, Introduction to Scanning Tunneling Microscopy, Oxford University Press, New York, 1993.
[14] F.J. Giessibl, Phys. Rev. B 56 (1997) 16010.